GAIT RECOGNITION USING SPARSE GRASSMANNIAN LOCALITY PRESERVING DISCRIMINANT ANALYSIS

Tee Connie, Michael Kah Ong Goh*, Andrew Beng Jin Teoh*[f]

*Faculty of Information Science and Technology, Multimedia University, Malaysia
[f]School of Electrical and Electronics Engineering, Yonsei University, Seoul, Korea

ABSTRACT

One of the greatest challenges for gait recognition is identification across appearance change. In this paper, we present a gait recognition method called Sparse Grassmannian Locality Preserving Discriminant Analysis. The proposed method learns a compact and rich representation of the gait images through sparse representation. The use of Grassmannian locality preserving discriminant analysis further optimizes the performance by preserving both global discriminant and local geometrical structure of the gait data. Experiments demonstrate that the proposed method can tolerate variation in appearance for gait identification effectively.

Index Terms— Gait recognition, locality preserving discriminant analysis, Grassmannian manifold, sparse representation

1. INTRODUCTION

Recently, gait recognition appears as a promising method for personal identification in surveillance applications. Gait recognition is a biometrics that identifies people by the way they walk. The suitability of gait recognition for surveillance application emerges from the fact that gait can be observed from a distance without requiring cooperation or even awareness of the people under observation. Other biometrics like face recognition might not work well for surveillance systems because people can disguise or hide their faces. Fingerprint and iris recognition are also not usable when the images are at too low a resolution. Although gait recognition has the potential to be deployed in visual surveillance to recognize people at a distance, the performance of the system suffers from deviation of the gait appearances in real world applications. Gait images of the same person might appear differently due to changes in view angle, clothing, carrying condition, walking speed and lighting factor. Studies showed that single-view gait recognition performance drops when the view angle changes [1–3].

Current approaches to gait recognition under various viewing angles can be classified into one of the three major categories: 1) extraction of view-invariant gait feature, 2) generation of 3D gait information, and 3) learning projection or mapping functions to transform gait features from various views into a common feature space. The first approach attempts to find gait features that are invariant to view changes like body part trajectories [4], estimated joint positions [5], and synthesis of a canonical side view [6]. Although these methods provide robust representations of the gait feature, they can only work with limited range of viewing angles and the accuracy can be affected by self-occlusion. The second approach integrates 3D information from multiple cameras to construct a gait model [7], [8], [9]. The drawback of these 3D analysis methods is that they require complicated setup of a calibrated multi-camera system. Besides, these methods demand complex and expensive computation which makes them unsuitable for real-time application. The third approach learns some mapping/projection function to normalize the gait features obtained from various viewing points to a shared feature space. Methods like view transformation model (VTM) [10], Multiview Subspace Representation (MSR) [11], and canonical correlation analysis [2] were introduced. These methods generate more stable gait features and they are less sensitive towards noise as compared to the methods in the first category. Furthermore, the methods in this category deploy simpler camera setup when compared to those in the second category.

In this paper, we propose a gait recognition method in the third category called Sparse Grassmannian Locality Preserving Discriminant Analysis (SGLPDA). This method extends the idea of Grassmannian learning proposed in [13], [14] by incorporating sparse representation (SR) in the algorithm. In gait recognition, the video of a walking person usually contains many variations. The gait data is thus distributed in a non-linear manifold. By formulating the gait recognition problem on the Grassmannian manifold, we can work in higher order data structure to harness the non-linear structure of the data and yet benefit from the conventional vector-based computation. With the incorporation of SR in our learning method, we can further attach semantic meaning to the gait data. The ability to uncover semantic information from the gait data is particularly useful when we need to recognize the gait appearances of the same person with vast variations. For example an image depicting a person wearing shirt and pants appears very differently than that of showing the person wearing long traveling cloak that covers most part of the body. SR allows us to represent these variations in a compact and representative basis which we found to be very useful in classifying gait features with various appearances. The contributions of the paper are two-folds: 1) construction of GLPDA to preserve both local geometrical structure and global discriminative information of the gait data; and 2) incorporation of SR in GLPDA to model the gait images effectively.

2. BACKGROUND

2.1. Grassmannian Manifold

The Grassmannian manifold $G(m, D)$ is a set of m-dimensional linear subspaces of the $\mathbb{R}^D$. It is computationally efficient to compute the distances between two points on the Grassmannian manifold using the principal angles [12]. Various distances have been defined based on the principal angles, and some well-known distances are the Binet-Cauchy, projection, correlation, and Procrustes distances. Among the various distances, the correlation measure, projection distance, and Binet-Cauchy distance are induced from positive definite kernels. This means we can define the corresponding kernels on the Grassmannian manifold based on these matrices. In this paper, the projection kernel and canonical correlation kernel are adopted as they are reported to provide good result [13], [14]. Given two points on a Grassmannian manifold, X_i and $X_j \in \mathbb{R}^{D\text{x}m}$, the similarity between the points is defined as:

$$k\_proj_{i,j} = \left\|X_i' X_j\right\|_F^2 \tag{1}$$

$$k\_cc_{i,j} = \max_{a_p \in span(X_i)} \max_{b_q \in span(X_j)} a_p^T b_q \tag{2}$$

subject to $a_p^T a_p = b_p^T b_p = 1$ and $a_p^T a_q = b_p^T b_q = 0, p \neq q$. *k_proj* denotes the projection kernel while k_cc signifies the canonical correlation kernel.

2.2. Sparse Representation (SR)

In the past few years, SR has proven to be a powerful tool for image processing, computational biology, statistics, pattern recognition and other applications [15–17]. Given a signal, or the column vector of an image in our case, $x_i \in \mathbb{R}^k$ and an overcomplete dictionary [18] with k bases, $X = [x_1, x_2, \ldots, x_n] \in \mathbb{R}^{n \times k}$, the goal of SR is to represent x_i using as few entries of X as possible. The objective function can be defined as follows:

$$\min \|S_i\|_0 \; s.t. \, x_i = XS_i \tag{3}$$

where S_i denotes the contribution of each x_j to reconstruct x_i. However, it is NP-hard to find the sparsest solution for Eq. (2) using l_0-minimization. As such, l_1-minimization is often used to solve the problem [18]. In practical applications, there might be noises in signal x_i. Therefore, the following optimization model is used to estimate S_i:

$$\min \|S_i\|_1 \; s.t. \, \|x_i - XS_i\|_2 < \varepsilon \tag{4}$$

where $\|\cdot\|_1$ is l_1-norm and ε is the error tolerant term.

3. PROPOSED APPROACH

A simple yet effective approach called Gait Energy Image (GEI) [19] is deployed to represent the gait feature. Given a gait sequence $\{I_t(i,j)\}_{t=1}^F$, where $I_t(i,j)$ is a pixel at position (i, j) in the image I_t, and F is the total number of frames in the gait sequence, GEI is defined as:

$$GEI(i,j) = \sum_{t=1}^{F} I_t(i,j)/F \tag{5}$$

One advantage of representing the gait feature using GEI is that we do not need to consider the underlying dynamics of the walking motion. This representation enables us to study the gait sequence from a holistic view by implicitly characterizing the structural statistics of the spatio-temporal patterns of the walking person.

3.1. Grassmannian Locality Preserving Discriminant Analysis (GLPDA)

The set of GEI images taken from the video sequence can be modeled as a collection of linear subspaces. We formulate the subspace matching problem on the Grassmannian manifold. By using a suitable Grassmannian kernel, the Grassmanian space can be treated in a similar manner as the Euclidean space. Conventional discriminant analysis tools like linear discriminant analysis (LDA) can thus be applied on the Grassmannian manifold to improve recognition accuracy [13], [14], [20]. LDA could not discover the local geometrical structure of the data manifold. Therefore, we used locality preserving discriminant analysis (LPDA) to reveal the local structure of the data. Different from traditional global linear methods such as LDA, LPDA utilizes both discriminant information and local geometry structure of the data manifold [21].

We formulate the gait recognition problem by using the graph embedding framework [22]. Let $G = \{V, W\}$ denotes an undirected weighted graph with vertices, V, and similarity matrix W. The elements in the similarity matrix are measures of the similarity for a pair of vertices. The values for W can be directly obtained from the output of the Grassmannian kernel. On the other hand, the diagonal matrix D and the Laplacian matrix L of the graph G are defined as $L = D - W$ where $D_{ii} = \sum_{j \neq i} W_{ij}$.

We want to find a mapping function $F{:}Y_i \rightarrow Z_i$ to map the points on the Grassmannian manifold, M, to a new manifold, M', so that the connected points of the within-class similarity matrix, $W_{w,ij}$, stay as close as possible while connected points of the between-class similarity matrix, $W_{b,ij}$, stay as distant as possible. To this end, we aim to optimize the following objective functions:

$$min \sum_{ij} (Z_i - Z_j)^2 W_{w,ij} \tag{6}$$

$$max \sum_{ij} (Z_i - Z_j)^2 W_{b,ij} \tag{7}$$

The objective function $W_{w,ij}$ incurs a heavy penalty if neighboring points Z_i and Z_j are mapped far apart while they are actually in the same class. Likewise, the objective function $W_{b,ij}$ incurs a heavy penalty if neighboring points Z_i and Z_j are mapped close together while they belong to different classes.

Suppose U is a projection matrix, $Z^T = U^T Y$, to realize the objective functions (6) and (7). By simple algebra manipulation, the objective function (6) can be reduced to:

$$\begin{aligned} &1/2 \sum_{ij} \left(Z_i - Z_j\right)^2 W_{w,ij} \\ &= 1/2 \sum_{ij} \left(U_i^T Y_i - U_j^T Y_j\right)^2 W_{w,ij} \\ &= \sum_i U_i^T Y_i D_{W,ii} Y_i^T U_i - \sum_{i,j} U_j^T Y_j D_{W,ij} Y_j^T U_j \\ &= \mathbf{U}^T \mathbf{Y} D_W \mathbf{Y}^T \mathbf{U}^T - \mathbf{U}^T \mathbf{Y} W_W \mathbf{Y}^T \mathbf{U}^T \end{aligned} \tag{8}$$

where D_w is a diagonal matrix given by $D_{w,ij} = \sum_j W_{w,ij}$. Similarly, the objective function (7) can be condensed to the following form:

$$\begin{aligned} &1/2 \sum_{ij} \left(Z_i - Z_j\right)^2 W_{b,ij} \\ &= 1/2 \sum_{ij} \left(U_i^T Y_i - U_j^T Y_j\right)^2 W_{b,ij} \\ &= \mathbf{U}^T (D_b - W_b) \mathbf{Y}^T \mathbf{U} \\ &= \mathbf{U}^T \mathbf{Y} L_b \mathbf{Y}^T \mathbf{U} \end{aligned} \tag{9}$$

where D_b is a diagonal matrix obtained through $D_{b,ii} = \sum_j W_{b,ij}$. Following the discussion in [21], the optimization problem reduces to finding:

$$\arg \max_{\substack{\mathbf{U} \\ \mathbf{U}^T \mathbf{Y} D_W \mathbf{Y}^T \mathbf{U} = \mathbf{1}}} \{\mathbf{U}^T \mathbf{Y} (\alpha L_B + (1-\alpha) W_W) \mathbf{Y}^T \mathbf{U}\} \tag{10}$$

where α is a constant and $0 \leq \alpha \leq 1$. The projection matrix $\mathbf{Y}$ that minimizes (10) is given by the maximum eigenvalue solution to the generalized eigenvalue problem:

$$(\alpha L_B + (1-\alpha) W_W) \mathbf{Y}\, \mathbf{U} = \boldsymbol{\lambda} \mathbf{Y} D_W \mathbf{Y}^T \mathbf{U} \tag{11}$$

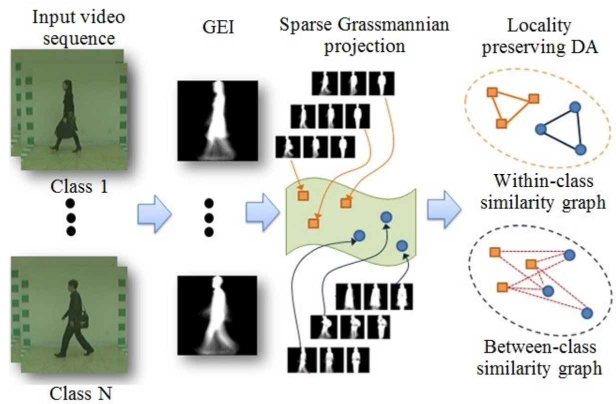

Fig. 1. Overview of GSLPDA.

3.2. Gait Recognition Using SGLPDA

In this section, we describe in detail how SR can be embedded in the GLPDA method. Fig. 1 depicts the steps required in the proposed method. Given sets of GEI images obtained using Eq. (5), we compute SVD over the image sets to obtain the corresponding subspaces $\{V_1, V_2, \ldots, V_n\}$ where $V_i \in \mathbb{R}^{Dxm}$ and D refers to the length of the gait feature while m signifies the number of images comprising the subspaces. After that, we apply a Grassmannian kernel to convert the subspaces into points on the Grassmannian manifold. To this end, we have tested two types of kernel functions namely the projection and canonical kernels [13], [14] given in Eq. (1) and (2). The output of the Grassmannian kernel, $\widehat{\mathbf{V}} = \{\hat{v}_1, \hat{v}_2, \ldots, \hat{v}_n\}$, is a $n \times n$ matrix. Next, we construct the between-class similarity graph, $W_{b,ij}$, and within-similarity graphs $W_{w,ij}$, by using SR. Suppose S_w is the sparse output estimated by Eq. (4) using the column vector of $\widehat{\mathbf{V}}$, the within-similarity graphs is defined as,

$$W_{w,ij} = \begin{cases} S_w(i,j), & \text{if } \hat{v}_i \in N_w(\hat{v}_j) \text{ or } \hat{v}_j \in N_w(\hat{v}_i) \\ 0, & \text{otherwise} \end{cases} \quad (12)$$

where $N_w(\hat{v}_i)$ is the set of k neighbors sharing the same label with $\hat{v}_i$. Similarly, the between-similarity graphs is defined as,

$$W_{b,ij} = \begin{cases} S_b(i,j), & \text{if } \hat{v}_i \in N_b(\hat{v}_j) \text{ or } \hat{v}_j \in N_b(\hat{v}_i) \\ 0, & \text{otherwise} \end{cases} \quad (13)$$

where S_b is the sparse output estimated by Eq. (4) using the column vector of $\widehat{\mathbf{V}}$ and $N_b(\hat{v}_i)$ is the set of k neighbors containing the neighbors having different labels than $\hat{v}_i$. We observe that large connecting weights are assigned to images resembling high similarities (e.g. images from the same person) and vice versa. Fig. 2 depicts some samples of within- and between-class similarity graphs learnt by SR for different scenarios (e.g. changes in view angles and clothing conditions). The graphs are represented using the "jet" colormap in Matlab which ranges from blue to red. Darker/cooler colors indicate lower values while brighter/warmer colors represent higher values. For example, the within-class similarity graphs shown in the second row of Fig. 2 are mostly covered in blue which implies that these graphs are very sparse.

Having constructed the within- and between-similarity graphs, we apply GLPDA to find the projection matrix $\mathbf{Y}$ by solving the eigenvalue decomposition problem in Eq. (11). Given the gallery image set is represented as $Z_G = \mathbf{Y}^T\widehat{V}_G$ where $\widehat{V}_G$ is the output of the Grassmannian kernel, and $Z_P = \mathbf{Y}^T\widehat{V}_P$ is the probe image set, we use k-nearest neighbor to measure the similarity between Z_G and Z_P.

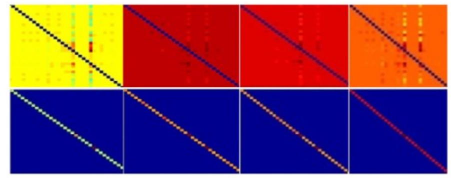
Fig. 2. The sparse between- (top) and within- (bottom) class similarity graphs learnt by SR for four different scenarios.

There are several benefits of applying SGLPDA on gait data. Firstly, SR does not require pre-determined parameters like the neighborhood size as compared to the k-nearest neighbor and ε-ball method in graph construction. This makes the method easier to use in practice. Secondly, we find that adaptive weight assignment is more effective than using off-the-shelf function like simple-minded graph because learning is performed by locally harvesting the intrinsic properties of the images [15]. This is useful to determine the appropriate combination of features that can enhance the recognition of gait images with different appearances.

4. EXPERIMENTS

4.1. Databases

The proposed method was tested on the CASIA gait database: Dataset B [23] and the OU-ISIR gait database: Dataset A and B [24]. The CASIA gait database is good for evaluating the effect of view variations on gait as it contains large number of subjects taken from different viewing angles. The CASIA gait database consists of 124 subjects captured from eleven different angles. The viewing angles range from 0^o to 180^o, separated by an interval of 18^o. There are ten walking sequences for each subject, with six samples containing subjects walking under normal condition, two samples with subjects walking with coats, and two samples with subjects carrying bags. Therefore, there are altogether 13,640 (10 x 11 x 124) gait sequences in the database. All the images are cropped and normalized to 120 x 120 pixels. On the other hand, the OU-ISIR gait database is suitable for assessing the influence of speed changes and clothing variations on gait. The OU-ISIR gait database: Dataset A contains 35 subjects captured from side view with speed variation from 2 km/h to 7km/h, at 1 km/h interval. There are two walking sequences for each speed level. Thus, there are 420 (2 x 6 x 35) gait sequences in this dataset. On the other hand, Dataset B is made up of 68 subjects acquired from side view with clothing variations. There are many clothing combinations in this dataset which include pants, half shirt, rain coat, skirt, and cap. All the images for the OU-ISIR database were cropped and resized to 128 x 88 pixels.

4.2. Results and Discussions

4.2.1. Evaluation on View Variations

The CASIA gait database was used to testify the performance of the proposed method under different view changes. For clear indication, each of the viewing angles $\theta = \{0^o, 18^o, \ldots, 180^o\}$ were labeled as $L_{view} = \{1, 2, \ldots, 11\}$. The eleven angles for each subject were modeled as a subspace for that individual. We randomly selected four gait sequences from each subject for the gallery set and the remaining for the probe set. All the eleven view angles were modeled as the subspace for each sample in the gallery and probe sets. The experimental results are shown in Table 1. We compared our method with [3] and [11]. Besides, we had also used simple-minded function to construct the within- and between-similarity graph in order to verify the effectiveness of SR. For this test, we followed the method in [13] and used binary values 0 and 1 for Eq. (12) and (13). The rank-1 recognition rate (R1RR) was used as the performance indicator. The correct match was counted when the sample in the probe set was the best match (top one) from the gallery set. When all the viewing angles were used to train the system, 100% R1RR could be achieved for all the methods except for MSR. This is encouraging as the proposed method is shown to possess cross-view capability. However, it is very difficult to get all the viewing angles for the subjects in real-life applications. As such, we reduced the number of viewing angles in the gallery set to simulate the scenario of "missing" cameras. For example, some surveillance cameras might not be present at certain positions or the cameras could not capture the subjects from certain angles. For this test, we took the first few view angles as the gallery set and the remaining views as probe set Based on the results in Table 1, we notice that the proposed method using CC kernel consistently yields good results. The effectiveness of SR has been verified in the experiments. The result shows that the proposed method has potential to tolerate missing views when there is not enough cameras to monitor an area.

Table 1. Evaluating the effect of view angle changes reported using rank 1 recognition rate (%). The abbreviations *G* and *P* stand for gallery and probe sets. SM refers to the simple-minded graph.

Experiment Setting	MSR [11]	Score Fusion [3]	SGLPD ACC Kernel	SGLPDA Proj Kernel	SM CC Kernel [13]*	SM Proj Kernel [13]*
G: All angles P: All angles	98.79	**100**	**100**	**100**	**100**	**100**
G: 1,2,3,4,5 P: 6,7,8,9,10	44.22	2.42	**64.51**	38.00	62.32	32.39
G: 1,2,3,4 P: 7,8,9,10	26.34	3.63	**40.32**	22.00	38.31	13.84
G: 1,2,3 P: 8,9,10	22.31	7.66	**33.46**	15.70	33.25	14.51

4.2.2. Evaluation on Clothing and Carrying Conditions

We conducted another experiment to assess the performance of the proposed method for clothing and carrying variations. The main purpose of this experiment is to simulate the condition in which suspects captured by the surveillance cameras are trying to masquerade themselves by wearing covers like rain coat or hat. This experiment is also useful to identify the ability of the proposed method to discriminate individuals who wear loose outfits like baggy pants and skirt (for ladies) which can obstruct the gait pattern from being observed properly. The CASIA and OU-ISIR gait databases were used for this evaluation. For the CASIA database, we took four normal gait sequences as the gallery set and two bags-carrying and two coats-wearing sequences as the probe sets. All the eleven viewing angles were applied in the test. As for the OU-ISIR database, six different clothing combinations were tested. Most of the clothing combinations were from types A (e.g. regular pants and parka) to M (e.g. baggy pants and down jacket) [24]. The clothes types were chosen such that we could get the largest possible variations for the test. Only 16 subjects were tested in this experiment because we could only identify 16 corresponding pairs between Dataset A, the normal walking sequence, and Dataset B, walking with clothing variations. Six sequences from Dataset A were used as the gallery set while the six sequences in Dataset B were used as the probe set. The results of the tests are shown in Fig. 3. We find that the variations in

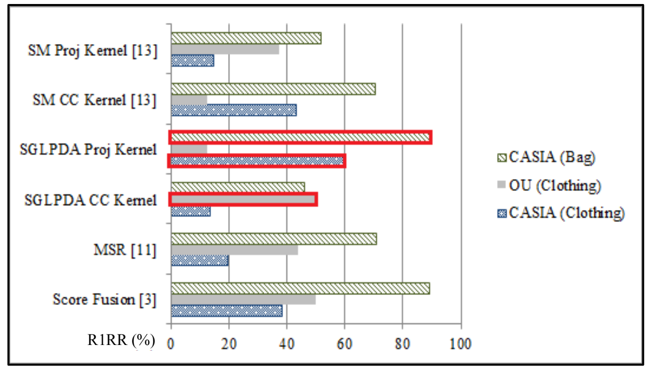

Fig. 3. Evaluating the effect of clothing and carrying conditions.

clothing alter an individual's appearance and make the problem of gait identification challenging. Nevertheless, the proposed method yield reasonable result and SR exhibits better performance over the other methods in this difficult identification task. Overall, the experimental result suggests that further investigation has to be carried out to study gait recognition with substantial clothing variation.

4.2.3. Evaluation on Walking Speeds

We have also conducted experiments to assess the effect of walking speed on gait. We are interested in this study as the suspect usually walks faster in order to leave the crime scene immediately. The OU-ISIR gait database was used for this evaluation. Using similar treatment as the view angles evaluation, we labeled the speed S = {2 km/h, 3 km/h, …, 7 km/h} as L_{speed} = {1, 2, …, 6}.The results are shown in Table 2. Unlike clothing variations, speed changes do not drastically affect the accuracy of gait identification. Therefore, the method can tolerate speed variations quite robustly.

Table 2. Evaluating the effect of varying walking speeds.

Experiment Setting	MSR [11]	Score Fusion [3]	SGLPDA CC Kernel	SGLPDA Proj Kernel	SM CC Kernel [13]	SM Proj Kernel [13]
G: All speeds P: All speeds	100	97.06	**100**	**100**	97.06	94.11
G: 1,3,5 P: 2,4,6	69.11	92.65	**94.11**	50.00	92.88	47.06
G: 1,3 P: 2,4	66.17	88.24	**94.11**	25.00	91.18	17.65

5. CONCLUSION

This paper presents a robust gait recognition method using SGLPDA. To the best of our knowledge, the application of SR on Grassmannian manifold has not been fully explored. We are the first to formulate the gait identification task using SR on the Grassmannian manifold. Experiment results suggest that the proposed method has potential for practical application as it demonstrates view- and speed-invariant capabilities.

6. ACKNOWLEDGEMENT

This research was partially supported by Ministry of Science and Technology (MOSTI), Malaysia, Ministry of Knowledge Economy (MKE), Korea, and Microsoft Research, under IT/SW Creative research program supervised by the NIPA (National IT Industry Promotion Agency)" (NIPA-2012-(2012-8-1813)).

7. REFERENCES

[1] S. Yu, D. Tan, and T. Tan, “A Framework for Evaluating the Effect of View Angle, Clothing and Carrying Condition on Gait Recognition,” in *18th International Conference on Pattern Recognition, 2006. ICPR 2006*, 2006, vol. 4, pp. 441 –444.

[2] K. Bashir, T. Xiang, and S. Gong, “Cross View Gait Recognition Using Correlation Strength,” 2010, pp. 109.1–109.11.

[3] R. Kawai, Y. Makihara, C. Hua, H. Iwama, and Y. Yagi, “Person Re-identification using View-dependent Score-level Fusion of Gait and Color Features,” presented at the Proc. of the 21st Int. Conf. on Pattern Recognition, 2012, pp. 2694–2697.

[4] F. Jean, R. Bergevin, and A. B. Albu, “Computing and evaluating view-normalized body part trajectories,” *Image and Vision Computing*, vol. 27, no. 9, pp. 1272–1284, Aug. 2009.

[5] M. Goffredo, I. Bouchrika, J. N. Carter, and M. S. Nixon, “Self-Calibrating View-Invariant Gait Biometrics,” *IEEE Transactions on Systems, Man, and Cybernetics, Part B: Cybernetics*, vol. 40, no. 4, pp. 997 –1008, Aug. 2010.

[6] A. Kale, A. K. R. Chowdhury, and R. Chellappa, “Towards a View Invariant Gait Recognition Algorithm,” in *Proceedings of IEEE Conference on Advanced Video and Signal Based Surveillance*, 2003, pp. 143–150.

[7] R. Bodor, A. Drenner, D. Fehr, O. Masoud, and N. Papanikolopoulos, “View-independent human motion classification using image-based reconstruction,” *Image Vision Comput.*, vol. 27, no. 8, pp. 1194–1206, Jul. 2009.

[8] G. Zhao, G. Liu, H. Li, and M. Pietikäinen, *3D Gait Recognition Using Multiple Cameras*. .

[9] Z. Zhang and N. F. Troje, “View-independent person identification from human gait,” *Neurocomputing*, vol. 69, no. 1–3, pp. 250–256, Dec. 2005.

[10] Y. Makihara, R. Sagawa, Y. Mukaigawa, T. Echigo, and Y. Yagi, “Gait recognition using a view transformation model in the frequency domain,” in *Proceedings of the 9th European conference on Computer Vision - Volume Part III*, Berlin, Heidelberg, 2006, pp. 151–163.

[11] N. Liu, J. Lu, Y.-P. Tan, and M. Li, “Set-to-set gait recognition across varying views and walking conditions,” in *Multimedia and Expo (ICME), 2011 IEEE International Conference on*, 2011, pp. 1 –6.

[12] G. H. Golub and C. F. van V. Loan, *Matrix Computations (Johns Hopkins Studies in Mathematical Sciences*, 3rd ed. The Johns Hopkins University Press, 1996.

[13] J. Hamm and D. D. Lee, “Grassmann discriminant analysis: a unifying view on subspace-based learning,” in *Proceedings of the 25th international conference on Machine learning*, New York, NY, USA, 2008, pp. 376–383.

[14] M. T. Harandi, C. Sanderson, S. Shirazi, and B. C. Lovell, “Graph embedding discriminant analysis on Grassmannian manifolds for improved image set matching,” in *Computer Vision and Pattern Recognition (CVPR), 2011 IEEE Conference on*, 2011, pp. 2705 –2712.

[15] J. Yang, J. Wright, T. S. Huang, and Y. Ma, “Image Super-Resolution Via Sparse Representation,” *IEEE Transactions on Image Processing*, vol. 19, no. 11, pp. 2861 –2873, Nov. 2010.

[16] K. Abhari, M. Marsousi, P. Babyn, and J. Alirezaie, “Medical image denoising using low pass filtering in sparse domain,” in *2012 Annual International Conference of the IEEE Engineering in Medicine and Biology Society (EMBC)*, 2012, pp. 114 –117.

[17] J. Wright, A. Y. Yang, A. Ganesh, S. S. Sastry, and Y. Ma, “Robust Face Recognition via Sparse Representation,” *IEEE Transactions on Pattern Analysis and Machine Intelligence*, vol. 31, no. 2, pp. 210 –227, Feb. 2009.

[18] J. F. Murray and K. Kreutz-Delgado, “Visual Recognition and Inference Using Dynamic Overcomplete Sparse Learning,” *Neural Comput.*, vol. 19, no. 9, pp. 2301–2352, Sep. 2007.

[19] J. Han and B. Bhanu, “Individual Recognition Using Gait Energy Image,” *IEEE Trans. Pattern Anal. Mach. Intell.*, vol. 28, no. 2, pp. 316–322, Feb. 2006.

[20] T. Wang and P. Shi, “Kernel Grassmannian distances and discriminant analysis for face recognition from image sets,” *Pattern Recognition Letters*, vol. 30, no. 13, pp. 1161–1165, Oct. 2009.

[21] D. Cai, J. Han, X. He, K. Zhou, and H. Bao, “Locality sensitive discriminant analysis,” *IJCAI*, vol. 2007, pp. 1713–1726.

[22] S. Yan, D. Xu, B. Zhang, H.-J. Zhang, Q. Yang, and S. Lin, “Graph Embedding and Extensions: A General Framework for Dimensionality Reduction,” *Pattern Analysis and Machine Intelligence, IEEE Transactions on*, vol. 29, no. 1, pp. 40 –51, Jan. 2007.

[23] “CASIA Gait Database.” [Online]. Available: http://www.cbsr.ia.ac.cn/english/Gait%20Databases.asp.

[24] Y. Makihara, H. Mannami, A. Tsuji, M. A. Hossain, K. Sugiura, A. Mori, and Y. Yagi, “The OU-ISIR Gait Database Comprising the Treadmill Dataset,” *IPSJ Trans. on Computer Vision and Applications*, vol. 4, pp. 53–62, Apr. 2012.